Dephasing-enabled triplet Andreev conductance

B. Béri
Instituut-Lorentz, Universiteit Leiden, P.O. Box 9506, 2300 RA Leiden, The Netherlands
(Received 12 March 2009; revised manuscript received 13 May 2009; published 17 June 2009)

We study the conductance of normal-superconducting quantum dots with strong spin-orbit scattering coupled to a source reservoir using a single-mode spin-filtering quantum-point contact. The choice of the system is guided by the aim to study triplet Andreev reflection without relying on half-metallic materials with specific interface properties. Focusing on the zero-temperature, zero-bias regime, we show how dephasing due to the presence of a voltage probe enables the conductance, which vanishes in the quantum limit, to take nonzero values. Concentrating on chaotic quantum dots, we obtain the full distribution of the conductance as a function of the dephasing rate. As dephasing gradually lifts the conductance from zero, the dependence of the conductance fluctuations on the dephasing rate is nonmonotonic. This is in contrast to chaotic quantum dots in usual transport situations, where dephasing monotonically suppresses the conductance fluctuations.

DOI: 10.1103/PhysRevB.79.245315 PACS number(s): 73.63.Kv, 74.45.+c, 85.75.−d, 03.65.Yz

I. INTRODUCTION

The triplet superconducting proximity effect[1–3] in half metals (fully polarized ferromagnets conducting only for one spin direction) has received considerable attention recently, both theoretically[4–11] and experimentally.[12–15] The mechanism behind the effect is the process of triplet Andreev reflection at the half-metal-superconductor interface.[2,4] The key ingredient that allows and influences this reflection process is provided by the magnetic properties of the interface between the half metal and the superconductor: it should have a magnetization that is misaligned from that of the half metal.[2,4] The role of such an interface is to break all the symmetries in spin space, thereby allowing for the spin rotations necessary for the triplet Andreev reflection. The properties of the interface, however, are not easy to manipulate in experiments, which is the reason why only a low proportion of half-metal-superconductor samples shows the behavior consistent with triplet Andreev reflection.[13–15] Here we study triplet Andreev reflection in a setup that is free of this difficulty. The setup consists of an Andreev quantum dot[16] (i.e., a quantum dot in contact with a superconductor) coupled to a normal source reservoir via a single-mode quantum-point contact (QPC) (see Fig. 1). Spin-orbit scattering in the quantum dot is assumed to be strong enough so that the direction of the spin is randomized in much shorter time than the typical time t_{dw} of the escape from the dot. This allows the dot to effectively play the role of the interface. The role of the half metal is played by the QPC, which is set to the spin-selective e^2/h conductance plateau using a parallel magnetic field.[17] (For simplicity, we assume that the Andreev conductance of the contact to the superconductor is much larger than e^2/h, which makes the transport properties insensitive to the details of this contact.)

A surprising feature of triplet Andreev reflection is that despite the randomized spin in the quantum dot, the conductance of such a fully phase-coherent, single-channel system vanishes in the zero-temperature linear-response regime.[11] While current can be passed through the system using finite voltages or temperature, it is natural to ask whether there is still a possibility for transport in the zero-temperature linear-response limit. A hint is given by noting that the vanishing zero-bias conductance can be seen as a destructive interference phenomenon resulting from the *coherent* addition of the different electron-to-hole amplitudes. (For complete destructive interference, a particular relation is needed between the contributing amplitudes; here this is provided by the electron-hole symmetry.) One, therefore, expects that relaxing the condition of full-phase coherence might enable the zero-bias triplet Andreev conductance to take nonzero values. In the remaining sections, our goal is to demonstrate that this is indeed the case by studying the behavior of the triplet Andreev conductance in the presence of dephasing in detail.

II. VOLTAGE PROBE AS A SOURCE OF DEPHASING

We introduce dephasing by coupling the quantum dot to an additional normal reservoir, which acts as a voltage probe.[18–22] A voltage probe draws no net current, but it absorbs and reinjects quasiparticles without a phase relationship, thereby destroying phase coherence. Dephasing due to

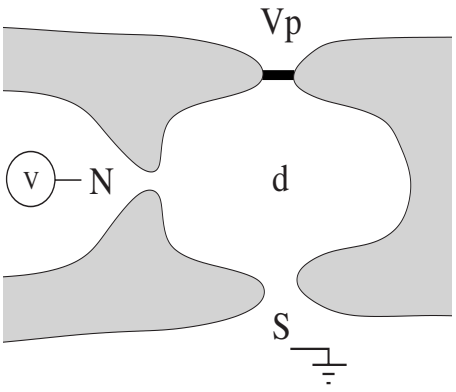

FIG. 1. Sketch of the setup studied in this paper. A normal-conducting chaotic quantum dot (d) coupled to a superconductor (s) via a many-mode contact, and to a normal source reservoir (n), held at an infinitesimal voltage V, via a single-mode, spin-filtering QPC. Dephasing is introduced by coupling the dot to a voltage probe (Vp) via a contact supporting N_ϕ modes with a tunnel barrier (black rectangle) of transparency Γ_ϕ per mode.

a voltage probe in normal-superconducting structures at zero temperature was studied in Refs. 23–25 for systems where no triplet Andreev reflection could occur. The contact to the voltage probe is characterized by the number of modes (including the spin degrees of freedom) N_ϕ and the tunnel probability per mode Γ_ϕ, which together determine the dephasing rate as $g_\phi = N_\phi \Gamma_\phi \delta/h$, where δ denotes the mean-level spacing of the quantum dot. We consider two limits, a voltage probe with a single-mode, spin-filtering contact $N_\phi = 1$, and a voltage probe with macroscopic number of modes $N_\phi \gg 1$. In the first case, the dephasing rate is controlled by the tunnel probability. In the second case, for $g_\phi \sim 1$, which will turn out to be the regime where the conductance behaves nontrivially, the transport properties depend on N_ϕ and Γ_ϕ only through their product, i.e., the dephasing rate.[22] The two limits considered here represent two types of voltage probes that appear in the context of spin-dependent quantum transport.[26] The probe $N_\phi = 1$ is a spin-conserving probe, while without further specification, the $N_\phi \gg 1$ can be either a spin-conserving or a spin-nonconserving voltage probe. For the systems studied in this paper, there is no need for further specification as the type of the voltage probe is unimportant due to the strong spin-orbit scattering in the quantum dot.

We formulate our problem within the framework of the scattering-matrix approach. The transport quantities of interest are expressed in terms of the scattering matrix S at the Fermi energy (the chemical potential of the superconductor), relating incoming and outgoing modes (including the electron-hole degrees of freedom) in the contacts to the normal reservoirs. The currents at the contact to the source and the voltage probe (denoted by N and Vp in Fig. 1, respectively) are given by[27,28]

$$I_\alpha = \frac{e^2}{h} \sum_{\alpha\beta} [N_\alpha \delta_{\alpha\beta} + \mathcal{R}^{he}_{\alpha\beta} - \mathcal{R}^{ee}_{\alpha\beta}] V_\beta, \tag{1a}$$

$$\mathcal{R}^{ij}_{\alpha\beta} = \mathrm{Tr}[(S^{ij}_{\alpha\beta})^\dagger S^{ij}_{\alpha\beta}], \tag{1b}$$

where $\alpha, \beta \in \{s, \phi\}$, with s labeling the source and ϕ labeling the voltage-probe contact, and the index e,h refers to electron and hole modes. The voltages V_β are measured from the chemical potential of the superconductor, which is assumed to be grounded. The voltage V_ϕ is determined by demanding that no current is drawn to the voltage probe $I_\phi = 0$. The conductance, defined by $G = V_s/I_s$, is given by

$$\frac{h}{e^2} G = 1 + \mathcal{R}^{he}_{ss} - \mathcal{R}^{ee}_{ss} - \frac{(\mathcal{R}^{he}_{s\phi} - \mathcal{R}^{ee}_{s\phi})(\mathcal{R}^{he}_{\phi s} - \mathcal{R}^{ee}_{\phi s})}{N_\phi + \mathcal{R}^{he}_{\phi\phi} - \mathcal{R}^{ee}_{\phi\phi}}, \tag{2}$$

where we substituted $N_s = 1$. Equation (2) is the starting point for our calculations. In what follows, we concentrate on systems where the motion inside the quantum dot is chaotic. We are interested in the statistics of the conductance, which we obtain using random-matrix theory[29] for the scattering matrix S.

III. DEPHASING DUE TO A SINGLE-MODE VOLTAGE PROBE

We first discuss the case of a voltage probe with $N_\phi = 1$. The calculational advantage of this case is that it allows for a problem with minimal dimension with the single-mode source contact and a single-mode voltage-probe contact resulting in a 4×4 scattering matrix. The parallel magnetic field, together with the strong spin-orbit scattering, places the quantum dot in the unitary symmetry class.[30] Consequently, the dot-superconductor system belongs to class D in the symmetry classification of Altland and Zirnbauer,[31] which translates to $S = \Sigma_1 S^* \Sigma_1$ as the only constraint for the scattering matrix, besides unitarity. (Σ_j denotes the jth Pauli matrix in electron-hole space.) Assuming that the contact to the source reservoir is ideal, the two single-mode QPCs can be characterized by the reflection matrix,

$$r = \begin{pmatrix} 0 & 0 \\ 0 & \sqrt{1-\Gamma_\phi} e^{i\Sigma_3 \xi}, \end{pmatrix}, \tag{3}$$

where the block structure reflects a grading according to the normal contacts [i.e., indices α and β in Eq. (2)] and ξ is the reflection phase shift for electrons at the voltage-probe contact. The statistical properties of the conductance follow from the distribution of the scattering matrix, which is given by the generalization of the Poisson kernel,[32]

$$P(S) \propto |\det(1 - r^\dagger S)|^{-3}. \tag{4}$$

The probability distribution is understood with respect to the invariant measure $d\mu(S)$ on the manifold $\mathcal{M}_D$, defined by $S = \Sigma_1 S^* \Sigma_1$ in the space of 4×4 unitary matrices. We parametrize S as

$$S = \begin{pmatrix} e^{i\psi_1}\sqrt{1-T}\mathbb{1}_2 & e^{i\psi_2}\sqrt{T}\tau \\ e^{-i\psi_2}\sqrt{T}\tau & e^{-i\psi_1}\sqrt{1-T}\mathbb{1}_2 \end{pmatrix} \begin{pmatrix} W & 0 \\ 0 & W^* \end{pmatrix}, \tag{5}$$

where $T \in (0,1)$, $\psi_1, \psi_2 \in (0, 2\pi)$, $W \in \mathrm{SU}(2)$, and $\tau = i\sigma_2$. (σ_j denotes the jth Pauli matrix in spin space.) The block structure in Eq. (5) corresponds to electron-hole grading. The above parametrization can be obtained from the polar decomposition introduced in the Appendix. Equation (5) implies that $\det(S) = 1$ and that the matrix $S^{he}(S^{he})^\dagger$ has a twofold degenerate eigenvalue T. This is true for the generic setups with vanishing linear conductance in the fully phase-coherent limit, i.e., if the closed Andreev quantum dot has no energy level at the Fermi energy.[11] (For a detailed discussion of this point we refer to the Appendix.) Using the Euler angle parametrization for W,

$$W = \begin{pmatrix} e^{-i(\varphi+\psi)/2}\cos(\theta/2) & -e^{i(\psi-\varphi)/2}\sin(\theta/2) \\ e^{i(\varphi-\psi)/2}\sin(\theta/2) & e^{i(\varphi+\psi)/2}\cos(\theta/2) \end{pmatrix},$$

$$(\varphi, \psi, \theta) \in [0, 2\pi] \times [0, 4\pi] \times [0, \pi], \tag{6}$$

the invariant measure on $\mathcal{M}_D$ is given by $d\mu(S) \propto \sin(\theta)$, and the conductance in units of e^2/h is

$$G(T, \theta) = 4\left(\frac{1}{T} + \frac{1}{\sin^2(\theta/2)}\right)^{-1}. \tag{7}$$

The distribution of the conductance is given by $P_{\Gamma_\phi}(G) = \int d\mu(S) P(S) \delta[G - G(T,\theta)]$, which can be reduced to

$$P_{\Gamma_\phi}(G) = \frac{\Gamma_\phi^3}{2G^2} \int_1^{4/G-1} dx \frac{2a^2 + b^2}{x^2(4/G - x)^2(a^2 - b^2)^{5/2}},$$

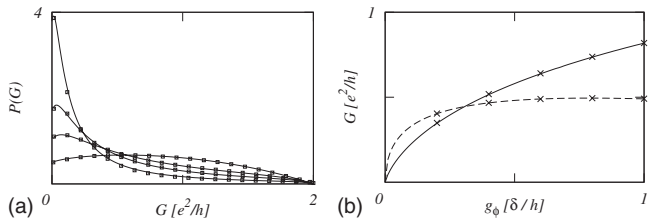

FIG. 2. Left panel: probability distribution [Eq. (8)] of the conductance for $N_\phi=1$, for various values of the dephasing rate $g_\phi=\Gamma_\phi\delta/h$. The curves, in order of decreasing maximum, correspond to $\Gamma_\phi=0.2$, 0.4, 0.6, and 1, respectively. The empty squares represent smoothed histograms obtained from 3000 numerically generated scattering matrices for each value of Γ_ϕ, for a system where the superconducting contact supports 50 propagating modes. Right panel: the average (solid line) and the standard deviation (dashed line) of the conductance as a function of g_ϕ. The crosses are results of the numerical simulation.

$$a = 1 - (1-\Gamma_\phi)\left(\frac{1}{4/G-x}+\frac{1}{x}-1\right),$$

$$\frac{b^2}{4} = (1-\Gamma_\phi)\left(1-\frac{1}{4/G-x}\right)\left(1-\frac{1}{x}\right) \tag{8}$$

for $0\le G\le 2$ and 0 otherwise. A closed-form expression can be given for $\Gamma_\phi=1$,

$$P_{\Gamma_\phi=1}(G) = 1 - \frac{2}{4-G} - \frac{G}{4}\ln\frac{G}{4-G}. \tag{9}$$

For $0<\Gamma_\phi<1$, we evaluated integral (8) numerically. The resulting distribution is shown in the top panel of Fig. 2 for several values of Γ_ϕ. In the absence of dephasing, the conductance vanishes, corresponding to $P_{\Gamma_\phi=0}(G)=\delta(G)$. With the gradual introduction of dephasing, G is enabled to take nonzero values, leading to a widening of the conductance distribution with increasing dephasing rate, eventually reaching distribution (9) for $\Gamma_\phi=1$. In the bottom panel of Fig. 2 we show the dependence of the average and the variance of the conductance on Γ_ϕ. While the average conductance increases monotonically with increasing dephasing rate, the variance increases to a maximum at $\Gamma_\phi\approx 0.8$, which is followed by a slight decrease. The finite value of the conductance fluctuations at $\Gamma_\phi=1$ (corresponding to the maximal dephasing for $N_\phi=1$) indicates that a single-channel voltage probe cannot lead to a complete loss of phase coherence; as we will see below, without phase coherence, the conductance fluctuations are suppressed back to zero. For weak dephasing $\Gamma_\phi\ll 1$, the conductance distribution is rapidly decaying away from $G=0$ and it has the scaling form $P_{\Gamma_\phi}(G)=f(G/\Gamma_\phi)/G$. This results in the dependence

$$\langle G^n\rangle \propto \Gamma_\phi^n, \quad \Gamma_\phi \ll 1 \tag{10}$$

for the nth moment of the conductance.

IV. DEPHASING DUE TO A MULTIMODE VOLTAGE PROBE

Now we turn to the case of the voltage probe with macroscopic number of channels $N_\phi\gg 1$. While it might be possible to make some analytical progress using the Poisson kernel distribution of Ref. 32 and following similar steps to the calculation of Ref. 22, we resort to a simpler approach and obtain the statistics of the conductance by generating an ensemble of scattering matrices numerically. The scattering matrix S is expressed in terms of the electron-scattering matrix,

$$S_N = \begin{pmatrix} r & t' \\ t & r' \end{pmatrix}, \tag{11}$$

of the normal region. Here r describes reflection from the dot through the normal contacts, r' describes reflection through the superconducting contacts, t corresponds to transmission to the superconducting, and t' corresponds to the normal contacts. The necessary blocks of S in electron-hole grading are given by[29,33]

$$S^{ee} = r - t'\sigma_2 r'^{*}\sigma_2(1+r'\sigma_2 r'^{*}\sigma_2)^{-1}t, \tag{12a}$$

$$S^{he} = -t'^{*}\sigma_2(1+r'\sigma_2 r'^{*}\sigma_2)^{-1}t. \tag{12b}$$

The scattering matrix S_N can be expressed using the statistical mapping,[34,35]

$$S_N = \sqrt{1-\Gamma} - \sqrt{\Gamma}\frac{1}{1-S_0\sqrt{1-\Gamma}}S_0\sqrt{\Gamma}, \tag{13}$$

where S_0 is unitary and Γ is a diagonal matrix containing the transmission probabilities of the contacts, with $\Gamma_{11}=1$ corresponding to perfect transmission through the single-mode QPC and $\Gamma_{jj}=\Gamma_\phi$ for $1<j\le N_\phi+1$ describing tunneling at the voltage probe. We took $\Gamma_{jj}=1$ for $j>N_\phi+1$, corresponding to the contact to the superconductor. The results do not depend on this choice as long as the Andreev conductance of the contact is much greater than e^2/h. Using the mapping ((13)), the distribution of S_N is obtained by taking S_0 from the circular unitary ensemble,[34,35] which we generated numerically.[36] For a mutual test of the program and the calculations, we first show results for $N_\phi=1$ in Fig. 2. As it is seen, the agreement between the calculation and the numerics is perfect. The conductance distribution in the limit $N_\phi\gg 1$ is shown in the top panel of Fig. 3 for several values of the dephasing rate g_ϕ. The distribution $P_{g_\phi}(G)$ initially widens from $P_{g_\phi=0}=\delta(G)$ with increasing g_ϕ and then it gradually narrows again to $P_{g_\phi=\infty}=\delta(G-G_{\rm class})$, where

$$G_{\rm class} = \left(\frac{1}{G_{\rm QPC}}+\frac{1}{G_{\rm NS}}\right)^{-1} \approx G_{\rm QPC} = 1 \tag{14}$$

is conductance of the single-mode QPC and the Andreev conductance of the superconducting contact in series in units of e^2/h. The dependence of the average and the variance of the conductance on g_ϕ is shown at the bottom panel of Fig. 3. While the average conductance increases monotonically to its classical value, the conductance fluctuations display nonmonotonic behavior, corresponding to the initial widening

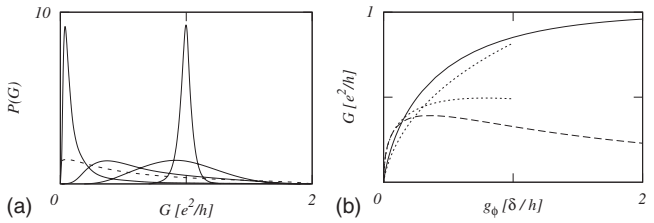

FIG. 3. Left panel: probability distribution of the conductance for $N_\phi \gg 1$, for different values of the dephasing rate g_ϕ. The solid curves, in order of increasing position G of the maximum, correspond to $g_\phi h/\delta = 0.05$, 0.5, 1.5, and 10, respectively. The curves are obtained by smoothing histograms from 3000 numerically generated scattering matrices for each value of g_ϕ, with $N_\phi = 100$, for a system where the superconducting contact supports 50 propagating modes. For comparison, we show the distribution for $N_\phi = 1$, $g_\phi h/\delta = 0.5$ (dashed line). Right panel: the average (solid line) and the standard deviation (dashed line) of the conductance as a function of g_ϕ. For comparison, the dotted lines show the corresponding functions for $N_\phi = 1$.

and the final renarrowing of the conductance distribution. Figure 3 also shows a comparison between the limits $N_\phi = 1$ and $N_\phi \gg 1$. For a given value of g_ϕ, the conductance distribution close to $G = 0$ is suppressed for $N_\phi \gg 1$, in contrast to the single-channel case, where $P(G=0)$ is finite. The average conductance increases faster for $N_\phi \gg 1$ toward its classical value, while the conductance fluctuations are suppressed compared to $N_\phi = 1$.

V. CONCLUSIONS

In summary, we have studied in detail how dephasing due to a voltage probe enables a nonzero value for the zero-temperature, zero-bias triplet Andreev conductance in Andreev quantum dots with a single-channel spin-filtering source-point contact. We focused on systems where the quantum dot is chaotic, and we obtained the full distribution of the conductance as a function of the dephasing rate for two limiting cases for the number of modes N_ϕ in the voltage-probe contact, $N_\phi = 1$ and $N_\phi \gg 1$. Compared to chaotic quantum dots in other transport situations, our findings for the conductance are quite unusual. Dephasing is known to monotonically suppress the conductance fluctuations in general.[21,29,37,38] In contrast, as dephasing gradually enables transport, the fluctuations of the triplet Andreev conductance are initially enhanced, which is followed by a suppression for strong dephasing; i.e., the overall dependence on the dephasing rate is nonmonotonic.

It is worthwhile to point out that in the $N_\phi \gg 1$ case, unlike Ref. 37, we did not intend to use the voltage probe to model dephasing processes intrinsic to the quantum dot since accounting for the temperature dependence of such processes would necessitate considering the effect of thermal smearing.[38] Instead, our results apply to the situation where the dephasing rate is controlled by a real, physically present voltage probe. Experimental control of the dephasing rate using a voltage probe was demonstrated very recently in the work of Roulleau *et al.*[39] This makes us believe that, in principle, it is realistic to test our predictions in experiments.

ACKNOWLEDGMENTS

This work originated from discussions with P. W. Brouwer. The author has also benefited from discussions with C. W. J. Beenakker. This research was supported by the Dutch Science Foundation NWO/FOM.

APPENDIX: ELECTRON-HOLE SYMMETRY, POLAR DECOMPOSITION, AND ANDREEV REFLECTION EIGENVALUES

The Andreev reflection eigenvalues T_j are the eigenvalues of the matrix $S^{he}(S^{he})^\dagger$. We prove here the consequences of electron-hole symmetry on these quantities and relate them to the condition of the absence of energy level of the closed Andreev quantum dot at the Fermi energy.

Theorem: At the Fermi energy, the degeneracy d_j of the Andreev reflection eigenvalue T_j is even if $T_j(1-T_j) \neq 0$ and $\det(S) = (-1)^{d_u}$, where d_u is the degeneracy of the unit Andreev reflection eigenvalue; if present, $d_u = 0$ otherwise. Furthermore, the scattering matrix at the Fermi energy can be decomposed in electron-hole grading as

$$S = \begin{pmatrix} U & 0 \\ 0 & U^* \end{pmatrix} \begin{pmatrix} \hat{R} & \hat{\rho}\hat{T} \\ \hat{\rho}\hat{T} & \hat{R} \end{pmatrix} \begin{pmatrix} V & 0 \\ 0 & V^* \end{pmatrix}, \tag{A1}$$

where U and V are unitary matrices,

$$\hat{R} = \bigoplus_j \sqrt{1-T_j}\,\mathbb{1}_{d_j}, \tag{A2a}$$

$$\hat{T} = \bigoplus_j \sqrt{T_j}\,\mathbb{1}_{d_j}, \tag{A2b}$$

and $\hat{\rho} = \oplus_j \rho_j$, where

$$\rho_j = \begin{cases} \mathbb{1}_{d_j} & \text{if } T_j(1-T_j) = 0 \\ \mathbb{1}_{d_j/2} \otimes \tau & \text{otherwise.} \end{cases} \tag{A3}$$

Proof: Following from the electron-hole symmetry $S = \Sigma_1 S^* \Sigma_1$, the scattering matrix has the block decomposition

$$S = \begin{pmatrix} S^{ee} & (S^{he})^* \\ S^{he} & (S^{ee})^* \end{pmatrix}. \tag{A4}$$

We start with the singular-value decomposition

$$S^{ee} = U' \hat{R} V', \tag{A5}$$

where U' and V' are unitary matrices. Using $(S^\dagger S)^{ee} = \mathbb{1}$ and $(SS^\dagger)^{ee} = \mathbb{1}$, one finds that

$$S^{he} = U'^* Z \hat{T} V'. \tag{A6}$$

Here Z is a block-diagonal unitary matrix,

$$Z = \bigoplus_j Z_j, \quad \dim Z_j = d_j. \tag{A7}$$

Substituting Eqs. (A5) and (A6) into $(S^\dagger S)^{he} = 0$ leads to

$$\sqrt{T_j(1-T_j)}Z_j = -\sqrt{T_j(1-T_j)}Z_j^T. \tag{A8}$$

For $T_j(1-T_j)\neq 0$, Z_j is antisymmetric and due to its unitarity $\det(Z_j)\neq 0$ from which it follows that d_j is even. Being antisymmetric and unitary, Z_j can be decomposed as[40,41]

$$Z_j = U_j^T \hat{\tau} U_j, \quad \hat{\tau} = 1_{d_j/2} \otimes \tau, \tag{A9}$$

where U_j is unitary. For $T_j=0,1$, Eq. (A8) is automatically satisfied without further requirements for Z_j. For the zero Andreev-reflection eigenvalue, if present, we can set $Z_j = U_j^T U_j$ with an arbitrary unitary matrix U_j; as for $T_j=0$, Z_j drops out from Eq. (A6). For the unit Andreev-reflection eigenvalue, if present, we write $Z_j = U_j^T U_j'$ with U_j and U_j' unitaries. Taken together, the matrix Z can be written as

$$Z = \bigoplus_j U_j^T \rho_j U_j', \tag{A10}$$

where $U_j' = U_j$ for $T_j \neq 1$. Writing U' and V' as

$$U' = U(\bigoplus_j U_j), \tag{A11a}$$

$$V' = (\bigoplus_j U_j'^{\dagger})V, \tag{A11b}$$

with U and V unitary, one finds

$$S^{ee} = U\hat{R}V \tag{A12a}$$

$$S^{he} = U^* \hat{\rho}\hat{T}V, \tag{A12b}$$

which gives the decomposition [Eq. (A1)] upon substitution in Eq. (A4). The decomposition [Eq. (A1)] satisfies the unitarity and electron-hole symmetry requirements; therefore, there are no further relations between matrices U and V. The result $\det(S)=(-1)^{d_u}$ follows straightforwardly. ■

Note that in Eq. (5) we assumed $\det(S)=1$, however, only $\det(S)=\pm 1$ follows from $S=\Sigma_1 S^* \Sigma_1$. We show below that this is a valid assumption in the generic situation that there is no energy level of the closed Andreev quantum dot at the Fermi energy. Using the channel coupled model employed in Ref. 31, the scattering matrix can be expressed as[29]

$$S_E = \frac{1+i\tilde{H}_E}{1-i\tilde{H}_E}. \tag{A13}$$

Here the Hermitian matrix $\tilde{H}_E = -\Sigma_1 \tilde{H}_{-E}^* \Sigma_1$ is a projection of $(\mathcal{H}-E)^{-1}$, where $\mathcal{H}$ models the closed Andreev quantum dot. If $\mathcal{H}$ has no zero eigenvalues, i.e., there is no level at the Fermi energy, the matrix $\tilde{H}_E$ can be taken at $E=0$ without complications. Following from the symmetry of $\tilde{H}_{E=0}$, the eigenvalues of S come in complex conjugate pairs; therefore, $\det(S)=1$. [If there is a level at the Fermi energy, an eigenvalue of $\tilde{H}_E$ can diverge as $E\to 0$ while another can tend to zero, leading to a $(1,-1)$ eigenvalue pair of S, and thereby to $\det(S)=-1$.] This result, together with $\det(S)=(-1)^{d_u}$, contains as a special case the finding of Ref. 11 that for a single-mode system, $S^{he}=0$ at the Fermi level if the closed Andreev quantum dot has no level at the Fermi energy. Indeed, for such a system, S is a 2×2 matrix; i.e., there is a single Andreev reflection eigenvalue. As it is singly degenerate, it can be only zero or unity and $\det(S)=1$ guarantees that it is zero. For the 4×4 matrix in Eq. (5), the degeneracy of the Andreev reflection eigenvalue also follows from $\det(S)=1$. If there was no degeneracy, the eigenvalues could be only a zero and a unit eigenvalue. This would mean that $\det(S)=-1$.

[1] F. S. Bergeret, A. F. Volkov, and K. B. Efetov, Phys. Rev. Lett. **86**, 4096 (2001).
[2] A. Kadigrobov, R. I. Shekhter, and M. Jonson, Europhys. Lett. **54**, 394 (2001).
[3] F. S. Bergeret, A. F. Volkov, and K. B. Efetov, Rev. Mod. Phys. **77**, 1321 (2005).
[4] M. Eschrig, J. Kopu, J. C. Cuevas, and G. Schön, Phys. Rev. Lett. **90**, 137003 (2003).
[5] V. Braude and Y. V. Nazarov, Phys. Rev. Lett. **98**, 077003 (2007).
[6] Y. Asano, Y. Tanaka, and A. A. Golubov, Phys. Rev. Lett. **98**, 107002 (2007).
[7] Y. Asano, Y. Sawa, Y. Tanaka, and A. A. Golubov, Phys. Rev. B **76**, 224525 (2007).
[8] S. Takahashi, S. Hikino, M. Mori, J. Martinek, and S. Maekawa, Phys. Rev. Lett. **99**, 057003 (2007).
[9] M. Eschrig and T. Löfwander, Nat. Phys. **4**, 138 (2008).
[10] A. V. Galaktionov, M. S. Kalenkov, and A. D. Zaikin, Phys. Rev. B **77**, 094520 (2008).
[11] B. Béri, J. N. Kupferschmidt, C. W. J. Beenakker, and P. W. Brouwer, Phys. Rev. B **79**, 024517 (2009).
[12] R. S. Keizer, S. T. Goennenwein, T. M. Klapwijk, G. Miao, G. Xiao, and A. Gupta, Nature (London) **439**, 825 (2006).
[13] V. N. Krivoruchko and V. Y. Tarenkov, A. I. D'yachenko, and V. N. Varyukhin, Europhys. Lett. **75**, 294 (2006).
[14] K. A. Yates, W. R. Branford, F. Magnus, Y. Miyoshi, B. Morris, L. F. Cohen, P. M. Sousa, O. Conde, and A. J. Silvestre, Appl. Phys. Lett. **91**, 172504 (2007).
[15] V. N. Krivoruchko and V. Y. Tarenkov, Phys. Rev. B **75**, 214508 (2007).
[16] C. W. J. Beenakker, Lect. Notes Phys. **667**, 131 (2005).
[17] R. M. Potok, J. A. Folk, C. M. Marcus, and V. Umansky, Phys. Rev. Lett. **89**, 266602 (2002).
[18] M. Büttiker, Phys. Rev. B **33**, 3020 (1986).
[19] M. Büttiker, IBM J. Res. Dev. **32**, 63 (1988).
[20] C. M. Marcus, R. M. Westervelt, P. F. Hopkins, and A. C. Gossard, Phys. Rev. B **48**, 2460 (1993).
[21] H. U. Baranger and P. A. Mello, Phys. Rev. B **51**, 4703 (1995).
[22] P. W. Brouwer and C. W. J. Beenakker, Phys. Rev. B **55**, 4695 (1997).
[23] N. Mortensen, A. Jauho, and K. Flensberg, Superlattices Microstruct. **28**, 67 (2000).
[24] T. Gramespacher and M. Büttiker, Phys. Rev. B **61**, 8125 (2000).

[25] M. Belogolovskii, Phys. Rev. B **67**, 100503(R) (2003).
[26] C. W. J. Beenakker, Phys. Rev. B **73**, 201304(R) (2006).
[27] Y. Takane and H. Ebisawa, J. Phys. Soc. Jpn. **61**, 1685 (1992).
[28] C. J. Lambert, V. C. Hui, and S. J. Robinson, J. Phys.: Condens. Matter **5**, 4187 (1993).
[29] C. W. J. Beenakker, Rev. Mod. Phys. **69**, 731 (1997).
[30] I. L. Aleiner and V. I. Fal'ko, Phys. Rev. Lett. **87**, 256801 (2001); **89**, 079902(E) (2002).
[31] A. Altland and M. R. Zirnbauer, Phys. Rev. B **55**, 1142 (1997).
[32] B. Béri, Phys. Rev. B **79**, 214506 (2009).
[33] C. W. J. Beenakker, Phys. Rev. B **46**, 12841 (1992).
[34] P. A. Mello, P. Pereyra, and T. Seligman, Ann. Phys. **161**, 254 (1985).
[35] P. W. Brouwer, Phys. Rev. B **51**, 16878 (1995).
[36] F. Mezzadri, Not. Am. Math. Soc. **54**, 592 (2007).
[37] P. W. Brouwer and C. W. J. Beenakker, Phys. Rev. B **51**, 7739 (1995).
[38] A. G. Huibers, S. R. Patel, C. M. Marcus, P. W. Brouwer, C. I. Duruöz, and J. S. Harris, Phys. Rev. Lett. **81**, 1917 (1998).
[39] P. Roulleau, F. Portier, P. Roche, A. Cavanna, G. Faini, U. Gennser, and D. Mailly, Phys. Rev. Lett. **102**, 236802 (2009).
[40] D. C. Youla, Can. J. Math. **13**, 694 (1961).
[41] J. Schliemann, J. I. Cirac, M. Kus, M. Lewenstein, and D. Loss, Phys. Rev. A **64**, 022303 (2001).